

Inhibition of GLO1 in glioblastoma multiforme increases DNA-AGEs, stimulates RAGE expression, and inhibits brain tumor growth in orthotopic mouse models.

Rahul Jandial¹, Josh Neman^{1,5}, Punrajit P. Lim², Daniel Tamae^{2,4,6}, Claudia M. Kowolik², Gerald E. Wuenschell², Sarah C. Shuck², Alexandra K. Ciminera^{2,4}, Luis R. De Jesus^{2,7}, Ching Ouyang³, Mike Y. Chen¹, and John Termini^{2*}

- ¹ Division of Neurosurgery, ²Department of Molecular Medicine, ³Center for Informatics, ⁴Irell and Manella Graduate School of Biological Sciences, City of Hope & Beckman Research Institute, 1500 East Duarte Road, Duarte, CA 91010; rjandial@coh.org (R.J.); plim@coh.org (P.L.); ckowolik@coh.org (C.K.); gwuenschell@coh.org (G.W.); sshuck@coh.org (S.S.); aciminera@coh.org (A.C.); couyang@coh.org (C.O.); mchen@coh.org (M.C.)
- ⁵ Department of Neurosurgery, Keck School Medicine, University of Southern California, 1975 Zonal Ave, Los Angeles, CA 90033; ybrahim@usc.edu (J.N.)
- ⁶ Department of Chemistry and Biochemistry, California State University, Northridge, 18111 Nordhoff Street, Northridge, CA 91330; daniel.tamae@csun.edu (D.T.)
- ⁷ Department of Chemistry, Texas A&M University, PO Box 30012, College Station, TX 77842; luis.dejesus@chem.tamu.edu (L.D.J.)
- * Correspondence: jtermini@coh.org (J.T.); Tel.: 626-218-8169; Fax: 626-930-5330

Figure S1: GLO1 expression in various cancer types. TCGA Pan-Cancer project RNA-Seq expression data (level 3 data using Illumina HiSeq platform) were applied to the analysis of GLO1 gene expression levels between primary tumors and normal tissues for different cancer types. Sixteen cancer types having data for both primary tumors and normal tissues ($N \geq 5$) were included in the analysis. Ten of the sixteen cancer types investigated, including GBM, showed statistically significant up-regulation of GLO1 expression. Standard box-plots were applied to visualize the expression distribution for each sample type. The red dots show the average values of each distribution. Fold changes (FC) in gene expression and number of samples (N) are indicated at the bottom. Statistical p-values between groups were calculated using Welch's t-test; $***p < 0.001$, $**p < 0.01$, $*p < 0.05$, n.s.: not significant. Legend keys for the abbreviated cancer types: BLCA: bladder urothelial carcinoma; BRCA: breast invasive carcinoma; CHOL: cholangiocarcinoma; COAD: colon adenocarcinoma; GBM: glioblastoma multiforme; HNSC: head and neck squamous cell carcinoma; KICH: kidney chromophobe; KIRC: kidney renal clear cell carcinoma; KIRP: kidney renal papillary cell carcinoma; LIHC: liver hepatocellular carcinoma; LUAD: lung adenocarcinoma; LUSC: lung squamous cell carcinoma; PRAD: prostate adenocarcinoma; READ: rectal adenocarcinoma; THCA: thyroid carcinoma; UCEC: uterine corpus endometrial carcinoma. GBM (also shown in Figure 1) is boxed blue.

Figure S2: Overall survival analysis based on GLO1 expression. Kaplan-Meier analyses of the overall survival in two brain cancer datasets based on GLO1 expression (Panel A: GSE13041 – GBM with

Affymetrix U95v2 platform; Panel B: GSE4271 – high-grade glioma with Affymetrix U133A platform). The analyses employ log-rank score tests to identify the optimal cut-point for best separation of patient groups. The grey dotted line shows the 3-year mark. The log-rank test *p*-value is shown in each panel.

Figure S3: RAGE (AGER) expression in various cancer types. Same as Figure S1, RAGE gene expression levels between primary tumors and normal tissues for different cancer types from TCGA Pan-Cancer project RNA-Seq data were delineated. Eight of the sixteen cancer types investigated, including GBM, showed statistically significant up-regulation of AGER expression.

Figure S4: Representative histological sections of patient GBM tissue obtained after surgery and stained for tumor stroma using hematoxylin-eosin (H&E) which revealed scattered pleomorphic nuclei consistent with the pathological criteria for malignancy.

Figure S5: Expression of GLO1 and RAGE in newly obtained human GBM specimens. Immunofluorescence in patient GBM tissues revealed strong GLO1 and RAGE expression (green). GFAP staining (red) indicates tumors of glial origin. Nuclei were stained with DAPI (blue). Hematoxylin-eosin (H&E) was used to stain for tumor stroma which revealed scattered pleomorphic nuclei consistent with the pathological criteria for malignancy. Scale bars represent 40 μ m.

Figure S6: LC-ESI-MS/MS chromatogram of (R,S) CE₂G. Representative MS/MS chromatograms in multiple reaction mode (MRM) for measurement of CE₂G in nuclear DNA. Top panel, natural abundance mass transitions at *m/z* 340→224 for *R* (~2 m) and *S* (~2.4 m) stereoisomers of CE₂G from T98 cells; bottom panel, isotopically enriched mass transitions for *R* and *S* CE₂G at *m/z* 345→229.

Figure S7: H&E brain slice of *p*-BrBzGSH(Cp)₂-treated mice 17 days post-implant. Hematoxylin-eosin (H&E) was used to stain for tumor stroma and identify the tumor region (dotted white line; also shown in Figure 6C).

Figure S8: GLO1 inhibition shows no toxicity in normal brain cells. Immunofluorescence in (A) vehicle and (B) *p*-BrBzGSH(Cp)₂ treated animals revealed no increase in apoptotic marker Caspase-3 in neurons (MAP2⁺/NeuN⁺), astrocytes (GFAP⁺), and oligodendrocytes (MBP⁺).

Figure S9: *p*-BrBzGSH(Cp)₂ treatment induces expression of GLO1 and RAGE. Inhibition of GLO1 with *S*-(*p*-bromobenzyl) glutathione dicyclopentyl ester [*p*-BrBzGSH(Cp)₂] elevated expression of GLO1 and various isoforms of the receptor for AGE (RAGE), esRAGE and fl-RAGE.

Figure S1.

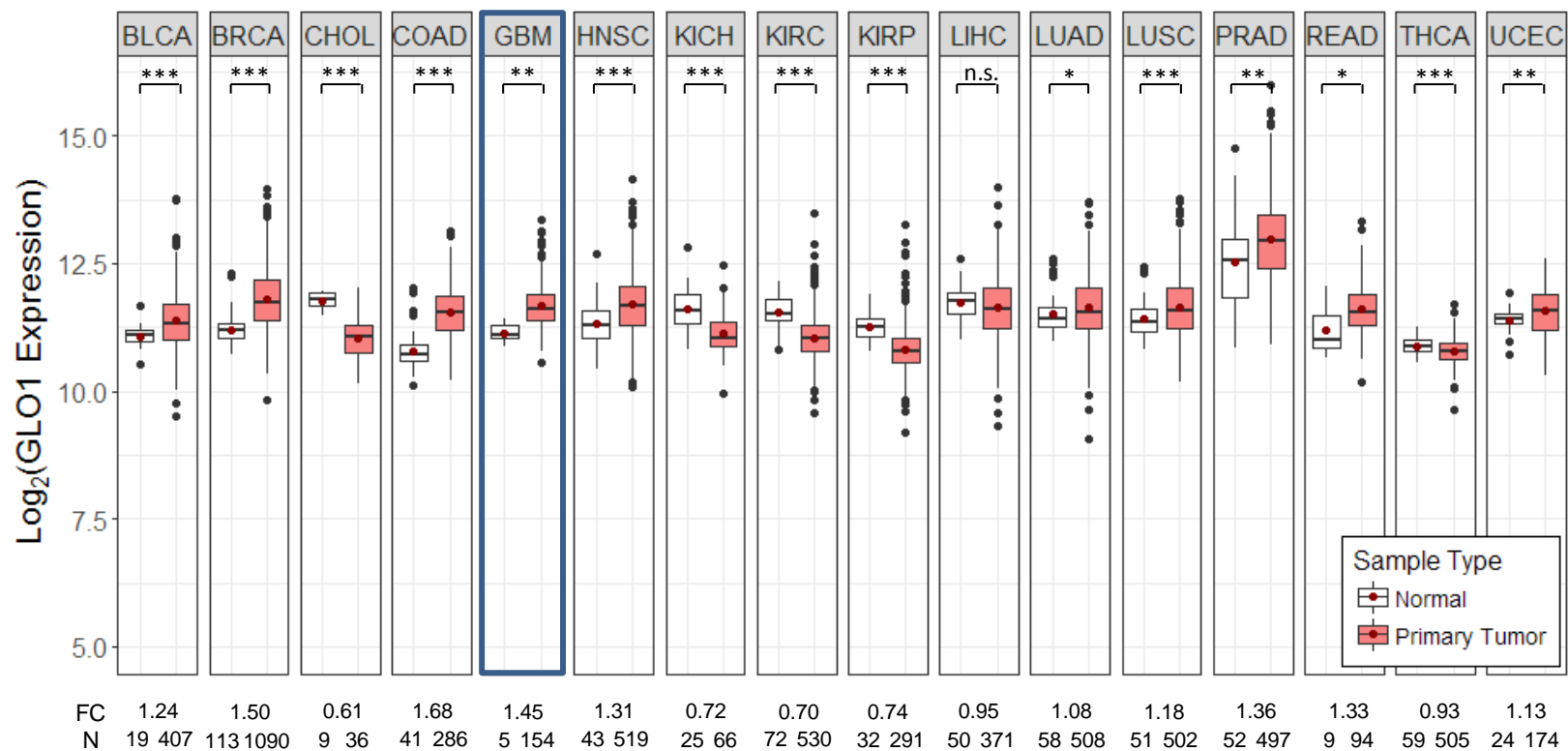


Figure S2

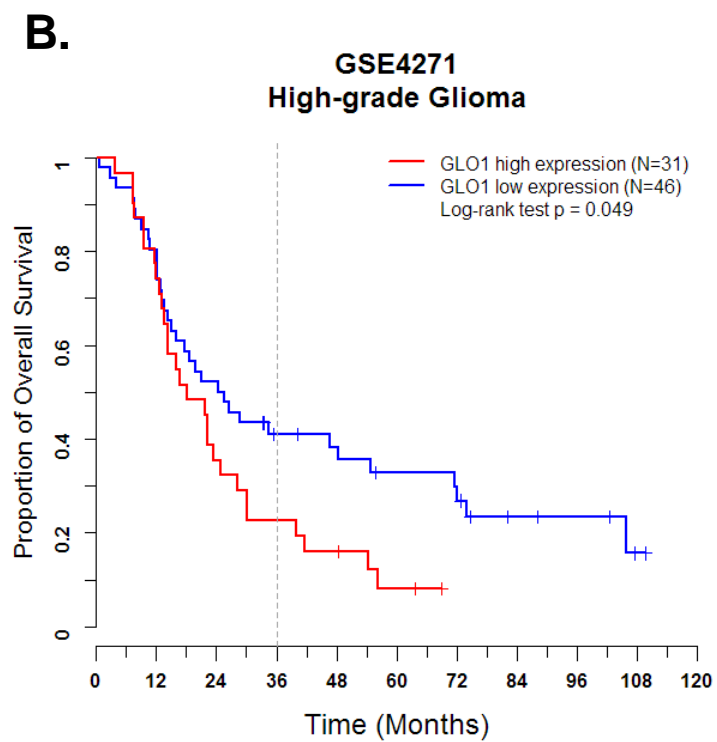
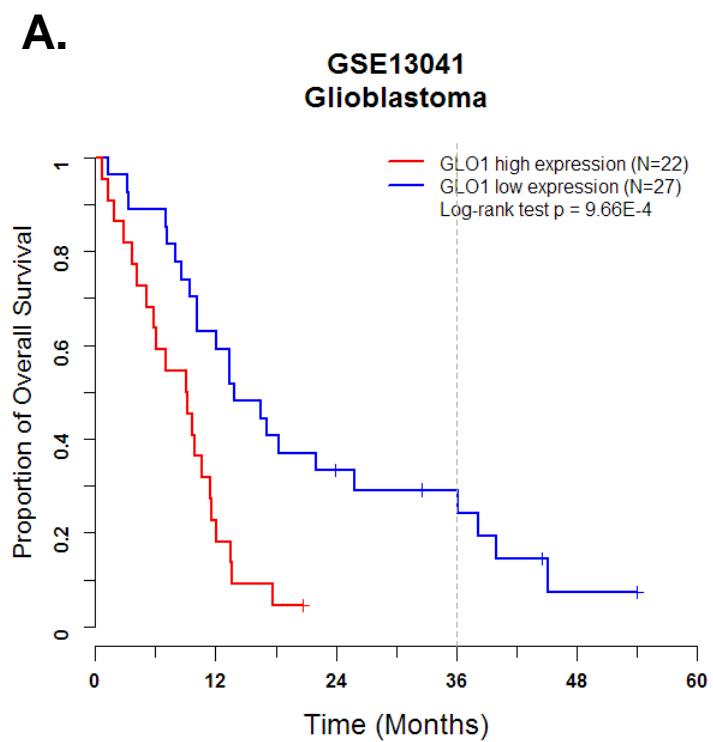


Figure S3.

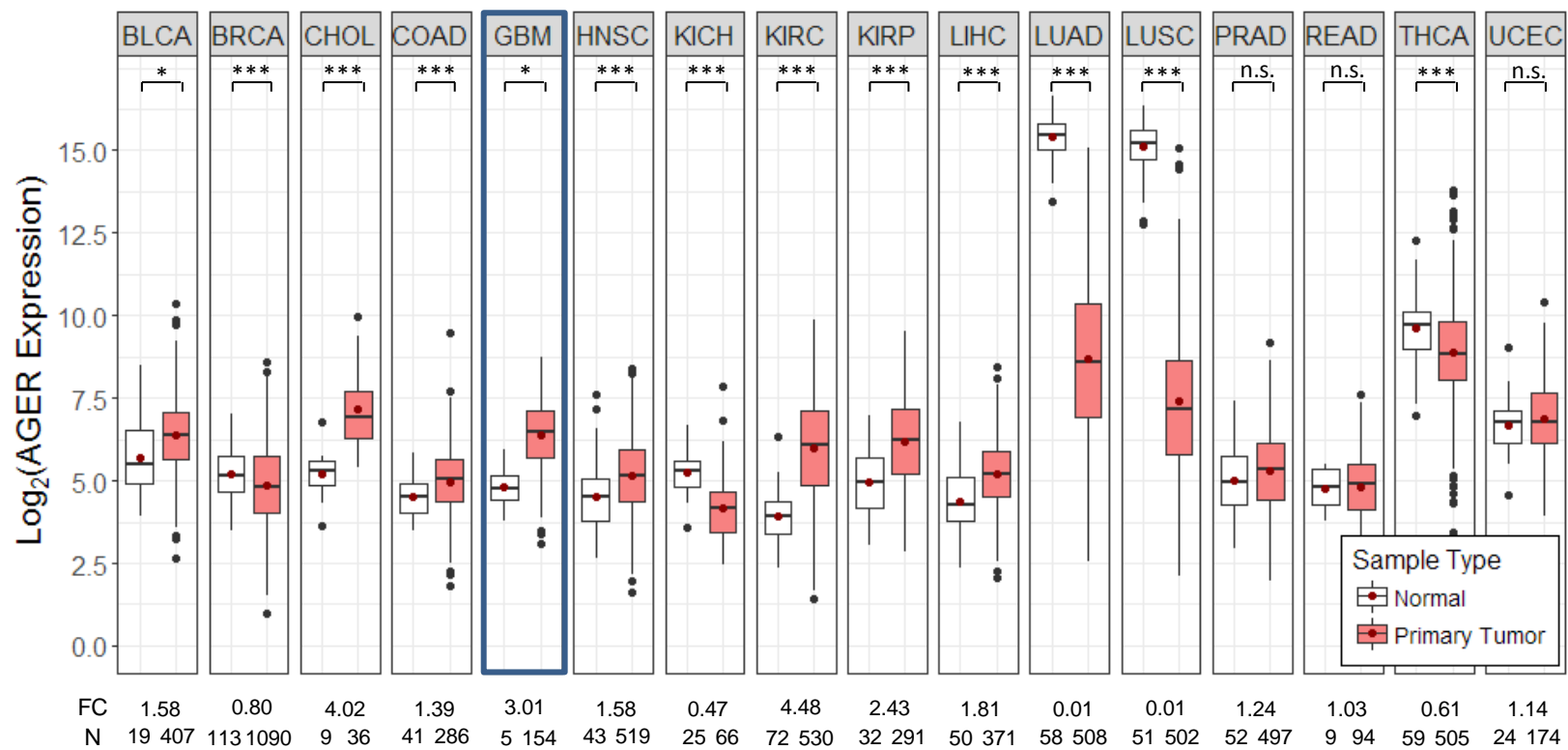


Figure S4.

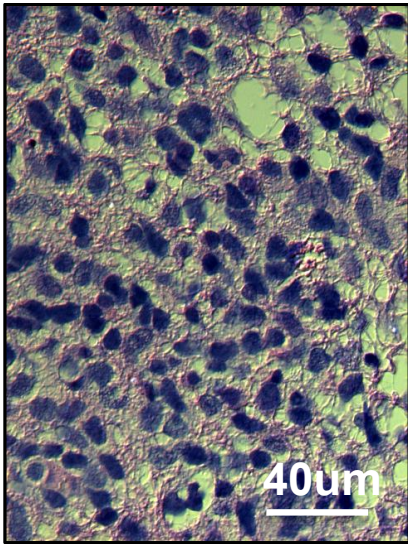


Figure S5.

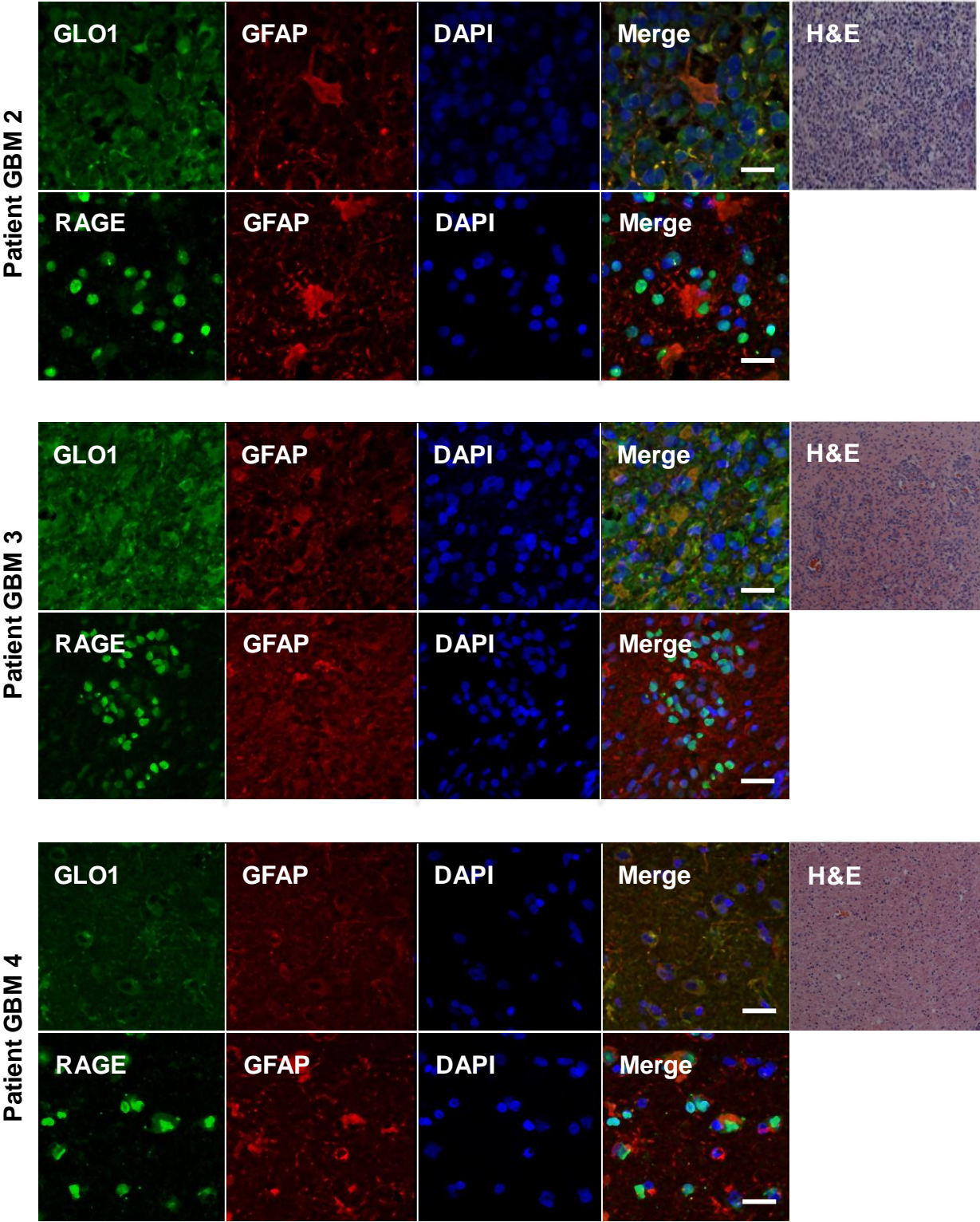


Figure S6.

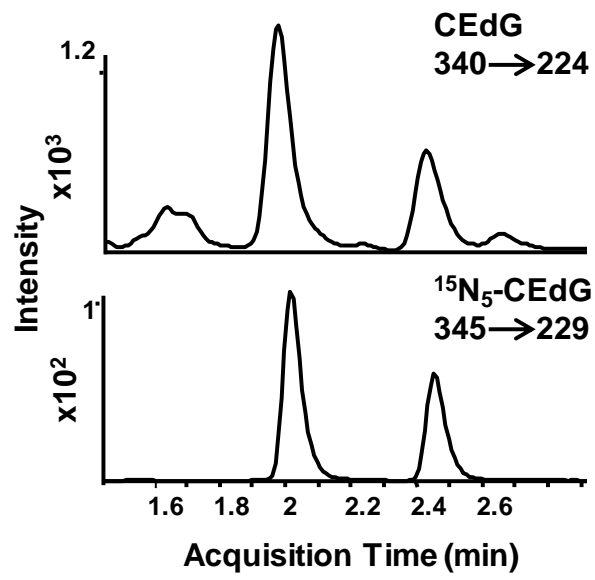


Figure S7

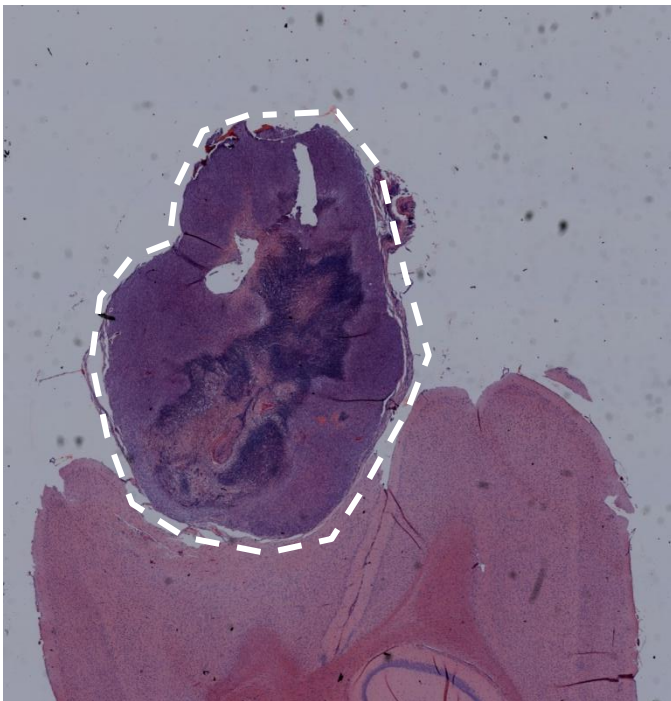


Figure S8.

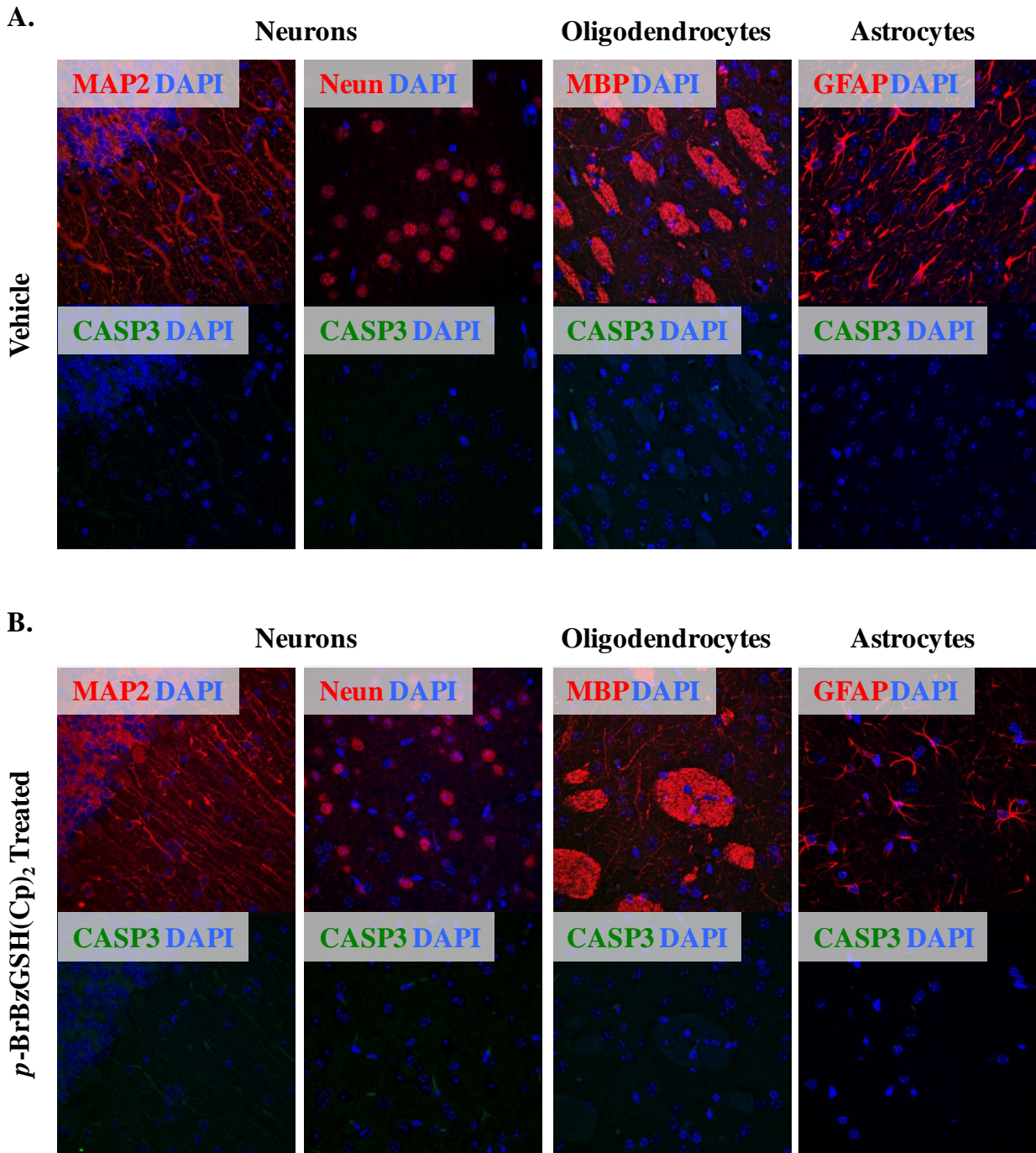


Figure S9.

